ELSEVIER

Thermal expansion of blood vessels in low cryogenic temperatures, Part II: Vitrification with VS55, DP6, and 7.05 M DMSO ☆

Jorge L. Jimenez Rios, Yoed Rabin *

Department of Mechanical Engineering, Carnegie Mellon University, Pittsburgh, PA 15213, USA

Abstract

As part of the ongoing effort to study the mechanical behavior of biological materials in cryopreservation processes, the current study focuses on thermal expansion during vitrification (vitreous in Latin means glassy). A new device is utilized in this study, which has been described in detail in the companion paper (Part I). The current study (Part II) focuses on measurements of vitrified blood vessels permeated with the cryoprotectants VS55, DP6, and DMSO. Data analysis in this study includes polynomial approximation of experimental results in the lower part of the cryogenic temperature range, where the material behaves as solid over a practical time scale. The study further includes a unified thermal expansion analysis throughout the entire cryogenic temperature range by compiling the current results with previously reported data. Finally, analysis of the glass transition temperature, based on thermal strain data is presented.
© 2006 Elsevier Inc. All rights reserved.

Keywords: Blood vessels; Thermal expansion; Vitrification; Cryopreservation; Continuum mechanics; Thermo-mechanical stress

Vitrification is an alternative to conventional cryopreservation of biological materials (vitreous in Latin means glassy), first suggested by Luyet [6], but applied successfully only in recent years [14,16,17]. Here, ice formation is completely prevented due to the presence of high cryoprotectant concentrations; viscosity increases exponentially with decreasing temperature, which eventually leads to an arrested state of the water molecules. No

appreciable degradation occurs over time in living matter trapped within a vitreous matrix, and vitrification is potentially applicable to all biological systems.

Vitrification is a relatively well-understood phenomenon, but its application to the preservation of biological systems is not without problems, since the high cryoprotectant concentration necessary to facilitate vitrification is potentially toxic. To limit the effects of toxicity, it is necessary to use the least toxic cryoprotectant and the minimum concentration that permits glass formation [1,2]. The cooling rate threshold above which glass forms (also known as the "critical cooling rate") is a physical property of the cryoprotectant and is inversely proportional

to the cryoprotectant concentration. In bulky mammalian tissues and large organs, the critical cooling rate is not always achievable at the center of the specimen, due to the thermophysical properties of the biological material and cryoprotectant, even when subjected to an extremely rapid cooling rate on the outer surface of the specimen. Moreover, when vitrification with a specific cryoprotectant is achievable in bulky tissues and organs, it is typically associated with large variations in temperature and cooling rate across the specimen. These variations lead to size limitations on vitrification, due to the tendency of the material to change its size with temperature.

The thermophysical property representing the tendency of the material to change its size with temperature is defined as the "thermal expansion," and the amount of expansion (or contraction) with respect to the original size is defined as "thermal strain." In the case of a non-uniform temperature distribution, a non-uniform tendency to expand (leading to a non-uniform thermal strain) develops. The mechanical stress originating from thermal strain is known as "thermo-mechanical stress." In general, thermo-mechanical problems relevant to vitrification belong to the field of continuum mechanics, where the specimen changes continually from a liquid to a solid-like material.

The observation that glass formation may be associated with structural damage is not new. Kroener and Luyet [5] studied the formation of fractures during vitrification of glycerol solutions in 10 ml vials, and the disappearance of fracturing during rewarming. In their short report, Kroener and Luyet [5] speculated on the conditions under which fractures are likely to occur. Following a similar line of research, Fahy et al. [3] studied the formation of fractures in propylene glycol solution, and in much larger containers of up to 1.5 L. They speculated that fractures can be prevented in large vitrifying systems if carefully handled.

The formation of macro-fractures in blood vessels has received a great deal of attention in the context of cryopreservation. Pegg at al. [9] performed an empirical investigation seeking the conditions under which macro-fractures occur in vascular tissues during cryopreservation, and they developed a protocol which prevents fracturing. It was found that fractures occurred as the temperature range of −150 to −120 °C was traversed during the rewarming phase of the process. Pegg et al. [9] succeeded in preventing fracturing when the warming rate in the temperature

range of −180 °C (storage temperature) and −100 °C was reduced to less than 50 °C/min.

A new imaging device termed a "cryomacroscope" has been presented recently, to study the likelihood of vitrification, crystallization, and fracture formation in bulky samples [12,15]. Initial studies were published on 1 ml samples of DP6 and VS55. The presence of fractures, as well as patterns in their position and orientation, were found to be dependent on the cooling rate and on the specific cryoprotectant cocktail. Fractures, if present, disappeared upon rewarming, although they were found to be sites for consequent crystallization. Computations which predict temperatures and mechanical stresses were used to explain observations of fracturing [15].

As part of the ongoing effort to study the mechanical behavior of biological material in cryopreservation processes, the current study focuses on thermal expansion of blood vessels during vitrification. A new experimental device for thermal expansion measurements of blood vessels in typical conditions to vitrification has been described in Part I of this paper [13]. The current paper (Part II) reports on thermal expansion results of blood vessels permeated with VS55, DP6, and 7.05 M DMSO, where VS55 and DP6 are cryoprotectant cocktails that draw significant interest in the development of vitrification technology, and 7.05 M DMSO has been established as a reference solution in previous studies [10]. Unified thermal expansion curves are further compiled based on the current results, and previously reported data from the upper part of the cryogenic temperature range [10]. Finally, data analysis in the current report includes the effect of glass transition on thermal expansion. To the best knowledge of the authors, the current study provides—for the first time—data on the thermal expansion of vitrifying biological materials in low cryogenic temperatures. The compilation, with previously developed data at the upper part of the cryogenic temperature range [10,11], provides for the first time, a comprehensive picture of the thermal expansion history of vitrifying biomaterial.

Material and methods

Artery sample preparation

Tissue specimens from goats (which were sacrificed for other purposes), were donated by a local slaughterhouse. No animals were sacrificed

specifically for the purpose of the current study. Artery segments were taken from either the main carotid artery (from smaller animals), or branches extending from the main carotid artery (from larger animals), were the emphasis was on the inner and outer diameters of the sample, to be compatible with the size of the cooling chamber. Tested samples had a diameter in the range of 4–6 mm, and length in the range of 41–50 mm. The wall thickness of the main carotid artery is about 1 mm, and the wall thickness of arteries extending from main carotid artery is about 0.5 mm. The wall thickness of the artery is expected to bear no effect on the thermal expansion in a stress free condition, as is the case in the current experimental setup. Samples were immersed in a phosphate-buffered saline (PBS) solution immediately after harvesting, and stored at 4 °C for a period between one and five days. This time period was selected due to practical time constraints of specimen availability and duration of experiments. The emphasis in this study is maintaining the structure of blood vessels segment; viability post-thawing is deemed unimportant in this context. Moreover, thermal expansion measurements were essentially the same, independent of the duration of immersion in PBS. Following protocol established in previous studies [7], specimens were stored in the cryoprotectant solution for 48 h before testing.

In total, one set of experiments on n specimens was performed for each of the cryoprotectants: DP6 ($n = 5$), VS55 ($n = 6$), and 7.05 M DMSO ($n = 5$). For purposes of protocol development and training, between three and five additional experiments were performed for each cryoprotectant, this data is not included in the current report. Two experimental runs were repeated on each sample, for a total number of $2n$ experiments for each of the above cryoprotectants. Between every two consecutive runs, the artery sample was removed from the chamber and the process of preparation of the measurement setup repeated itself. The reason for repeated experiments on the same sample was to identify whether the thermal expansion property is affected by the number of cooling cycles. The reason for repeated preparations between consecutive experiments is to eliminate possible systematic errors due to preparation errors with the sample.

DP6 is a cocktail of 234.4 g/L DMSO (3 M), 228.3 g/L propylene glycol (3 M), and 2.4 g/L Hepes in EuroCollins solution. VS55 is a cocktail of 242.1 g/L DMSO (3.1 M), 168.4 g/L propylene glycol (2.2 M), 139.6 g/L formamide (3.1 M), and 2.4 g/L Hepes in EuroCollins solution. The two cocktails are similar, with the exception of the exclusion of formamide from DP6. In return, the DP6 contains a higher concentration of propylene glycol. The mass of DMSO present in a 7.05 M solution is the same as the total mass from all the cryoprotectants present in VS55, hence it is used as a reference. The DP6 and VS55 cocktails have been prepared by Cell and Tissue Systems, Inc., Charleston, SC.

Data analysis of a vitrifying material

Fig. 1 schematically illustrates the dependency of thermal strain in temperature. Segment A–B is the upper part of the cryogenic temperature range, in which the material behaves like liquid from continuum mechanics considerations (i.e., where shear stress cannot develop without flow of the material). Results for VS55, DP6, and various concentrations of DMSO have been reported previously for that range, in the absence [10] and presence [11] of blood vessels and muscle specimens. Segment C–D is the lower part of the cryogenic temperature range, in which the vitrified material behaves like solid from continuum mechanics considerations (i.e., shear stress does not lead to flow of the material in the relevant time scale); the current study is aimed at measurements in this temperature range. Segment B–C is an interpolated range between the previously measured data (segment A–B), and data from the current study (segment C–D). The material can be considered neither solid nor liquid along the B–C segment.

As illustrated in the inset in Fig. 1, segment C–D can further be subdivided into two segments, above (C–G) and below (G–D) the glass transition temperature range, T_G. The reason for the monotonically increasing thermal strain (or contraction) with cooling, is that the molecules tend to rearrange closer to one another, in order to minimize intra-molecular forces (associated with minimum energy configuration). However, viscosity increases dramatically with the decrease in temperature, where the viscosity is typically modeled as exponentially dependent on the decrease in temperature. When the viscosity reaches a significantly high value, the molecules are trapped and cannot move fast enough to cope with the imposed intra-molecular forces. The temperature range at which this process takes place is know as the "glass transition temperature range,"
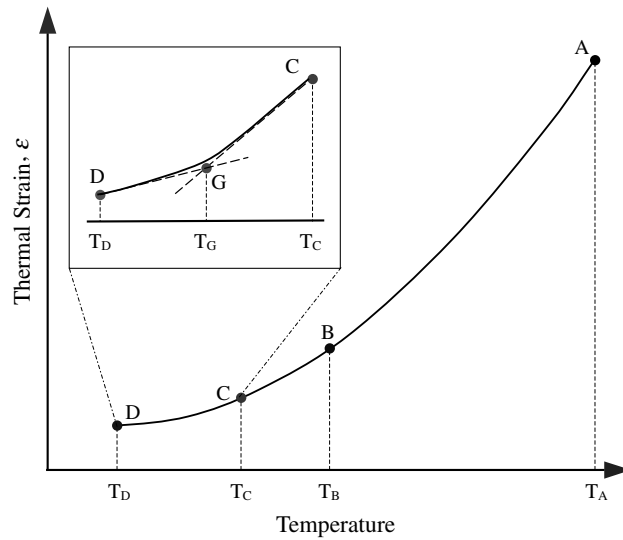
Fig. 1. Schematic illustration of the dependency of the thermal strain in temperature, where (A and B) is the range in which the material behaves like liquid, (B and C) is an interpolated range, (C and D) is the range in which the vitrified material behaves like solid for the purpose of the current study, and point G is the glass transition temperature, derived from thermal expansion considerations.

and the imaginary point at which the asymptotes to the thermal strain outside of this region meet is known as the "glass transition temperature." If the glassy material is maintained at a constant temperature, molecules will eventually move to their minimum energy state (i.e., locations), in a process known as "structural relaxation." The typical time constant for structural relaxation is proportional to the viscosity and, therefore, increases exponentially with the decrease in temperature. While structural relaxation may take a few minutes at a few degrees below the glass transition temperature, it may take an impractically long time at lower temperatures.

Note that there are alternative definitions to the glass transition temperature, which are also derived from the same exponentially-increasing viscosity effect [13]. Other definitions of the glass transition temperature are commonly associated with heat transfer measurements using calorimetric techniques [13]. In continuum mechanics analyses, T_G is frequently defined as the temperature at which viscosity reaches a value of 10^{13} poise (10^{12} Pa·s) [13].

A closer view of the expected thermal strain around the glass transition temperature is schematically illustrated in Fig. 2. In order to illustrate the thermal strain process along the ideal curve, a thought experiment is assumed in which the cooling rate decreases exponentially. The process starts with a very rapid cooling rate, in order to suppress crystallization and promote vitrification. As the
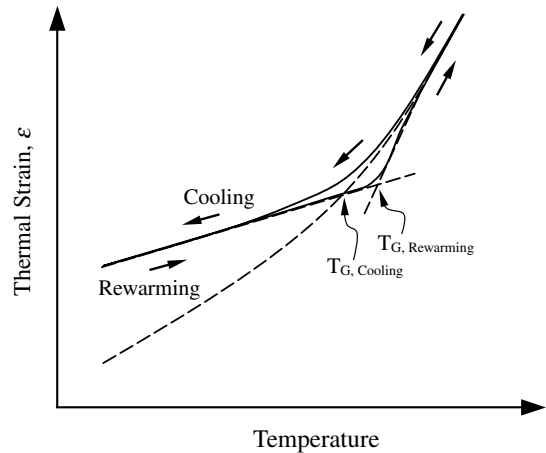

Fig. 2. Schematic illustration of the dependency of the thermal strain in temperature around glass transition [13].

process progresses, the cooling rate is decreased, inversely proportional to the viscosity value, in order to maintain the conditions for structural relaxation. At a practical cooling rate however, a deviation from the ideal curve will occur due to the structural trapping effect addressed above, which corresponds to the glass transition temperature during cooling, $T_{G,cooling}$. The glass transition temperature is not an intrinsic physical property, but decreases with the decreased cooling rate when approaching glass transition. The thermal expansion during cooling and rewarming is expected to be similar at very low temperatures, where structur-

al relaxation is insignificant. As the material re-warmed (and the viscosity decreases), a temperature range is reached at which the material regains its ability to flow, and structural rearrangements occur rapidly; this temperature range is associated with glass transition temperature during rewarming, $T_{G,rewarming}$. The temperature difference between $T_{G,cooling}$ and $T_{G,rewarming}$ is rewarming rate-dependent.

Data analysis in this study is performed in the following order: (i) best-fit polynomial approximation of thermal strain in the lower part of the cryogenic temperature range (T_D–T_C), where its slope is the thermophysical property of thermal expansion; (ii) best-fit polynomial approximation of a unified thermal strain curve in the entire range of temperature (T_D–T_A), based on compilation of the current data, previously reported data, and interpolation between the two data sets; and (iii) estimation of the glass transition temperature based on thermal strain data during cooling and subsequent rewarming.

Thermal expansion in lower cryogenic temperatures

Thermal strain data was compiled from experimental data on the elongation of the specimen and the cooling chamber, using the same mathematical formulation and system calibration presented in the previous paper [4]. While the experimental data in the previous paper refer to a solid material in the entire temperature range of measurements, the upper limit below which the vitrified material can be considered solid (and results can be consider valid) is yet to be established. For this purpose, Fig. 3 presents typical strain results obtained for a blood vessel specimen permeated with VS55. In contrast to the high repeatability below T_C in Fig. 3, repeatability virtually does not exist above the same temperature. Note that the specimen tends to contract during cooling, applying an upwards vertical force on the glass cylindrical rod of the telescopic tubing (Figs. 1 and 2 in [4]). Above T_C, the specimen yields to this force and the strain does not show monotonic contraction, but rather an unpredicted behavior. During rewarming, on the other hand, the force of gravity on the glass cylindrical rod assists the natural elongation, and the strain curve becomes monotonic in the entire temperature range. Below T_C, the thermal strain is calculated in the same manner described in [4].

The thermal strain, ε, is an integral property (the integral of the thermal expansion coefficient with respect to temperature), which is dependent on the initial condition (or a reference point). A variation in the upper temperature limit T_C was observed between consecutive experiments, which exceeded $\pm 10\,°C$ in some cases. In order to increase the statistical significance of the polynomial approximation of the thermal strain, $\hat{e}$, data analysis is based on n separate experiments under similar conditions. Since each experiment starts at a slightly different initial temperature, the approximation of $\hat{e}_j$ from a specific experiment j ($j = 1, \ldots, n$) may need to be
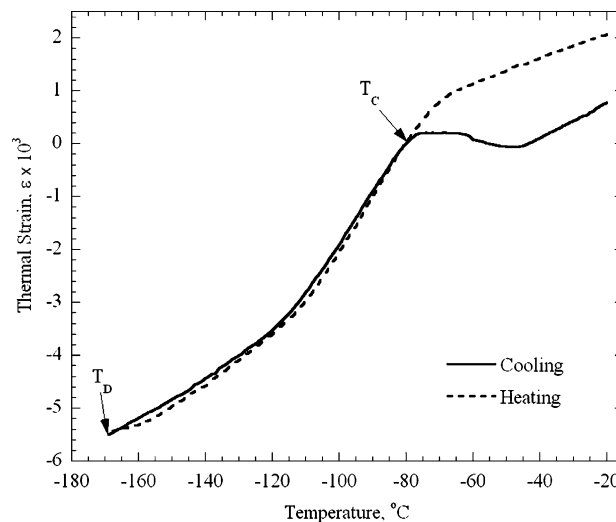

Fig. 3. Thermal strain measured during cooling and subsequent rewarming of an artery specimen permeated with VS55.

shifted in ε direction on the ε–T plane, so that data sets overlap. For this purpose, the approximation $\hat{e}_k$ ($k = j$, $j = 1, \ldots, n$) is arbitrarily selected as a reference. Next, an approximation of a second experiment is selected $\hat{e}_j$ ($j \neq k$, $j = 1, \ldots, n$), and all data points are shifted by a constant value $\Delta \hat{e}_j$, such that optimization parameter F_j is minimized:

$$F_j = \sum_i \left[\hat{e}_k - \left(\hat{e}_j - \Delta \hat{e}_j \right) \right]^2. \qquad (1)$$

This process is repeated for the entire set of experiments ($j \neq k$, $j = 1, \ldots, n$), where each experiment requires a different value of $\Delta \hat{e}_j$. Finally, a polynomial approximation $\hat{e}_j$ is calculated based on all shifted experimental data from all experiments combined.

Compilation of the unified thermal expansion curve

Thermal expansion in the upper part of the cryogenic temperature range has been presented previously [10,11] (segment A–B in Fig. 1), while thermal expansion in the lower part of this range is presented in the current report (segment C–D in Fig. 1). To make this data useful, the experimental data from both reports have been compiled, to provide one curve of thermal strain throughout the entire cryogenic range (termed the "unified curve"; segment A–D in Fig. 1). Note that the thermal strain in segment B–C is unmeasured.

Strain values were calculated from the established polynomial approximation in segment A–B [11] at 1 °C intervals, starting with zero strain at point A. Next, strain values were calculated in segment C–D (current study) at 1 °C intervals, starting with zero strain at point C. A best-fit polynomial approximation was calculated in the entire cryogenic range, with the requirement of minimum on the sum of the squared errors:

$$F = \sum_{i=1}^{n} \left[\hat{e}_{AD,i} - \hat{e}_{AB,i} \right]^2$$
$$+ \sum_{j=1}^{m} \left[\hat{e}_{AD,j} - \left(\hat{e}_{CD,j} + \Delta \hat{e}_{CD} \right) \right]^2, \qquad (2)$$

where $\hat{e}_{AD}$ is the unified polynomial approximation, $\hat{e}_{AB}$ is the available polynomial approximation in segment A–B, n is the number of data points in segment A–B, $\hat{e}_{CD}$ is the polynomial approximation in segment C–D, m is the number of data points in segment C–D, and $\Delta \hat{e}_{CD}$ is a shift of all data points in segment C–D, in order to make it compatible with segment A–B (zero initial strain at room tempera-

ture). Since both polynomial approximations in segments A–B and C–D are of a second order, the unified curve was also chosen to be of a second order. Since the shift $\Delta \hat{e}_{CD}$ is not known, its value was optimized to yield a minimum on F (which has only one minimum).

Estimation of the glass transition temperature

The glass transition temperature in this study is defined as the intersection of two asymptotic lines starting from points C and D, respectively. Starting from point C, the first three data points closest to point C are selected, the coefficients of a best-fit linear approximation are calculated, and the coefficient of determination, R^2, is recorded. This calculation is repeated many times, while gradually increasing the number of participating data points in the best-fit approximation, until the value of R^2 falls below a threshold of 0.995. While the R^2 value of 0.995 is deemed adequate to represent an asymptotic line in the current study, other values could be selected as well. (Similar analysis with an R^2 value of 0.999 yielded essentially the same results, which are not presented in this report.) Next, the same process of asymptotic line approximation is repeated, this time starting from point D. Finally, the glass transition temperature, T_G, is estimated as the intersection of the two asymptotic lines.

Results and discussion

The repeatability in strain measurements using the new experimental system has been demonstrated in Fig. 3. In order to verify uniformity in temperature along the blood vessel, a few experiments were performed with three thermocouples attached to the blood vessel specimen, one at the center and one at each end.

Fig. 4 presents the best-fit polynomial approximations of the thermal strain for VS55, DP6, and 7.05 M DMSO, with reference at −85 °C (approximation coefficients are listed in Table 1). It can be seen that the difference in thermal strain between VS55 and DP6 is about 4% of the full range of presentation, and both are lower by about 20% compared with 7.05 M DMSO.

Compilation of the unified curve

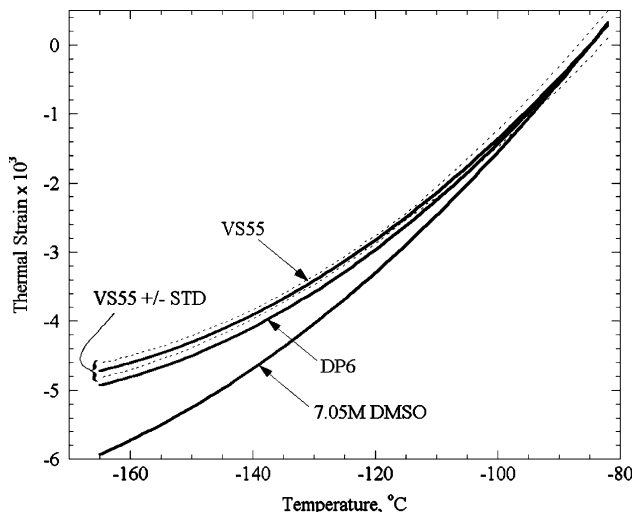Figs. 5–7 present the unified curves of thermal strain for the various cryoprotectants. It can be seen

Fig. 4. Thermal strain of artery specimens permeated with DP6 ($n = 5$), VS55 ($n = 6$), and 7.05 M DMSO ($n = 5$), with a reference temperature of −85 °C. The coefficients of polynomial approximation are listed in Table 1.

from Fig. 5 that, while no interpolation is needed between the two temperature ranges of measurements, the slope on both sides of the border between the two temperature ranges overlap. The significance of this observation is that while completely different devices and experimental protocols were employed in each temperature range, the resulting thermal expansion appears to match very accurately. This observation gives a high level of confidence in the results of both independent studies. Due to toxicity, the concentration of 7.05 M DMSO is far too high for cryopreservation (much lower concentrations of DMSO are mixed in the cryoprotectant cocktails VS55 and DP6). However, the use of 7.05 M DMSO as a reference solution is critical for the data comparison between the different experimental systems, as discussed above.

A significant interpolation range is observed in Figs. 6 and 7 for VS55 and DP6, respectively. In this range, neither the experimental systems presented previously [10,11] for the upper part of the cryogenic temperature, nor the system presented in the current study for the lower part of the cryogenic temperature, can produce experimental data with a good degree of certainty. The width of this gap is, to a large extent, associated with the maximum obtainable cooling rate in the previous system [10,11], where DP6 shows the highest critical cooling rate and 7.05 M DMSO the lowest rate. Nevertheless, it can be seen from those figures that a second order polynomial approximation for the unified thermal strain curve falls within the uncertainty

range of experimental data, which leads to a high level of confidence in data analysis.

Estimation of the glass transition temperature

With reference to Table 2, it can be seen that the thermal expansion coefficient of the vitrified material changes in the range of 41 to 68% upon glass transition, depending on the cryoprotectant, and whether it is measured during cooling or rewarming. The change in thermal expansion is lower during cooling than during rewarming in the range of 8 to 12%.

Observations on silica glasses suggest that the glass transition temperature during cooling is lower than during rewarming [13], as illustrated in Fig. 2. A similar trend was observed for 7.05 M DMSO and DP6, where the difference in T_G between cooling and rewarming is less than one standard deviation. The opposite effect was observed for VS55, but its significance is not established since the difference in glass transition between cooling and rewarming is much smaller than one standard deviation in temperature estimation for all the cryoprotectants measured in this study.

As addressed above, the glass transition temperature is dependent on the cooling rate [13]. In the range of cooling rates tested (Table 2), no such dependency could be observed. It could be expected that an order of magnitude increase in cooling rate would affect the glass transition to the order of 1 °C [13]. It appears that the range of cooling rates

Table 1
Coefficients of best-fit polynomial approximation of thermal strain, $\varepsilon = a_2T^2 + a_1T + a_0$, and the thermal expansion, $\beta = 2a_2T + a_1$, where R^2 is the coefficient of determination, T_B is the temperature above which the material can be considered liquid, T_C is the temperature below which the material can be considered solid for the purpose of the current study, and T_D is the minimum temperature achieved in an experiment (See also Fig. 1)

Solution	Temperature range (°C)	$a_0 \times 10^3$	$a_1 \times 10^4$	$a_2 \times 10^7$	R^2	n	T_B range	T_C range	T_D range	Source
VS55	−63.6 to 19.4	−3.711	2.081	9.425	0.9690	8	−82.5 to −57.0	n/a	n/a	[11]
	−165.3 to −82.5	—	1.785	4.781	0.9941	6	n/a	−90.1 to −75.1	−170.3 to −159.6	Current study
	−165.3 to 19.4	−3.652	1.911	5.312	0.9994	—	n/a	n/a	n/a	Current study
DP6	−40.5 to 19.2	−4.447	1.653	10.41	0.9984	6	−43.0 to −38.5	n/a	n/a	[11]
	−167.2 to −85.1	—	1.893	5.114	0.9847	5	n/a	−99.8 to −75.5	−175.3 to −163.4	Current study
	−167.2 to 19.2	−4.321	1.564	3.825	0.9997[b]	—	n/a	n/a	n/a	Current study
7.05 M DMSO	−93.1 to 18.8	−4.895	1.995	6.127	0.9976	6	−97.5 to −87.5	n/a	n/a	[11]
	−167.7 to −93.1	—	1.849	4.434	0.9669	5	n/a	−93.1[a]	−174.2 to −163.5	Current study
	−167.7 to 18.8	−4.939	1.890	4.796	0.9996	—	n/a	n/a	n/a	Current study

[a] Data in this range overlaps with data at the upper range ($T_D > T_B$); polynomial approximation was best-fitted for 7.05 M DMSO up to the average value of T_B.

[b] T_B of −34 °C is assumed when best fitting the unified curve for DP6, which is the freezing temperature at slow cooling rates.

applied in the current study is too narrow for a definitive observation of this kind, but higher cooling rates cannot be obtained in the current setup.

The glass transition temperature calculated in this study is found to be in very good agreement with literature data, measured with a differential scanning calorimetry (DSC). When comparing, it should be remembered that the DSC device measures the change in internal energy, while the current system measures the corresponding structural changes. Furthermore, since the change in internal energy occurs over a temperature range, and since there are alternative ways of representing this range with a single temperature value [8], (i.e., the glass transition temperature), it is not necessary that both techniques yield the same value. Nevertheless, the good agreement in measured glass transition temperature between DSC analysis and thermal strain analysis in the current study, enhances the level of confidence in the sensitivity of the new device and technique.

Finally, it is emphasized that the new experimental system is tailored to measure thermal expansion of vitrifying biomaterials, where the system tissue-cryoprotectant behaves as a composite material in the continuum mechanics sense. In the process of cooling, the tissue structure contains the cryoprotectant in a specific geometry (the tissue) until it reaches temperatures low enough to behave as a solid; it is in this temperature range that measurements of thermal expansion and glass transition are conducted. Unfortunately, to the best of our knowledge, no literature data on comparable systems in cryogenic temperatures is available for comparison. Furthermore, it is not possible to measure the glass transition of the pure cryoprotectant in the current system.

Summary

As part of the ongoing effort to study the mechanical behavior of biological material in cryopreservation processes, the current study focuses on thermal expansion of vitrified blood vessels. The cryoprotectant solutions under investigation are VS55, DP6, and DMSO, and the analysis combined newly developed data in lower cryogenic temperatures, with recently published data at higher cryogenic temperatures. To the best of our knowledge, this is the first attempt to study the thermal expansion of vitrified biomaterial throughout the entire cryogenic temperature range relevant to
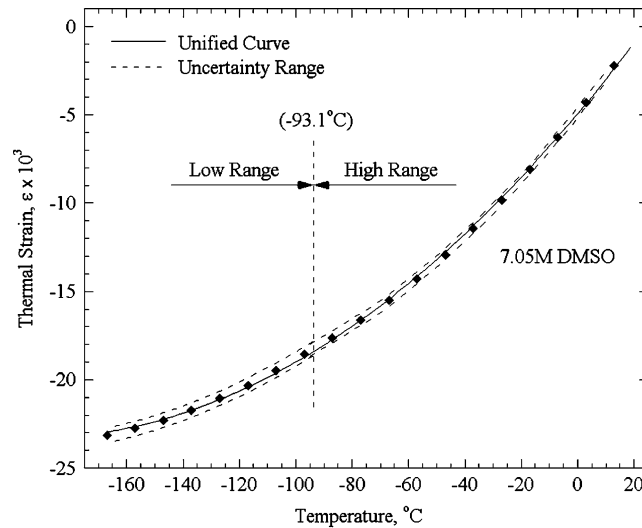
Fig. 5. Unified thermal strain curve of blood vessels permeated with 7.05 M DMSO.
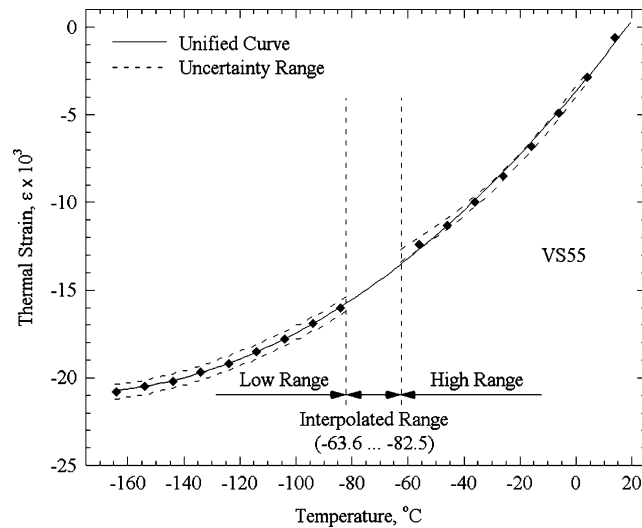

Fig. 6. Unified thermal strain curve of blood vessels permeated with VS55.

cryopreservation. Data analysis includes thermal strain, thermal expansion, and the effect of glass transition on this property.

In an effort to estimate the thermal expansion of DP6 and VS55 throughout the entire cryogenic temperature range, an interpolation technique has been employed to bridge the temperature gap between the previously reported data and current measurements. Such an interpolation technique was not required for 7.05 M DMSO, which has a greater tendency to form glass. A very good agreement in thermal expansion coefficient (i.e., the slope of the thermal strain) was found in the overlapping range of temperature of the two studies. This observation gives a high level of confidence in the devices, results, and techniques of data analysis in both independent studies.

The thermal expansion coefficient shows a decrease in the range of 41 to 68% upon glass transition, depending on the cryoprotectant. The change in thermal expansion is lower during cooling than during rewarming in the range of 8 to 12%. Analysis of glass transition temperature based on thermal expansion results and DSC studies are found to be in good agreement. No cooling rate dependency of the glass transition temperature was observed in the obtainable rates in the current experimental system.
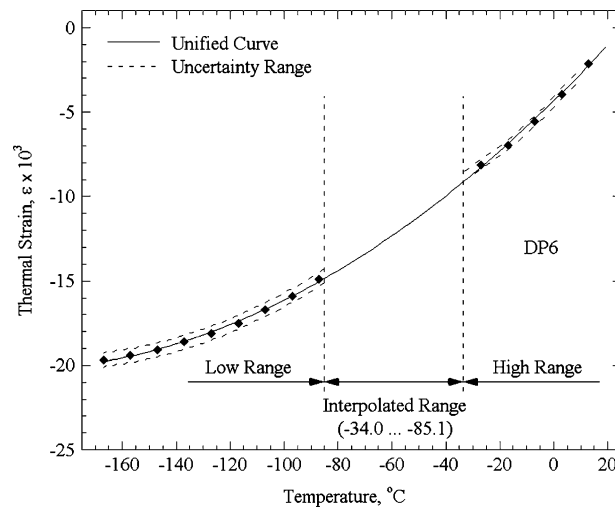
Fig. 7. Unified thermal strain curve of blood vessels permeated with DP6.

Table 2
Glass transition temperature, T_G, defined as the intersection of two asymptotic lines starting from points C and D in Fig. 1, respectively

	$\beta_{CG} \times 10^6$ (°C^{-1})	$\beta_{GD} \times 10^6$ (°C^{-1})	β_{CG}/β_{GD}	T_G (°C)	H (°C/min)	$T_{G,DSC}$ (°C)	n
VS55							
Cooling	85.7 ± 7.7	41.8 ± 3.2	0.49	-119.8 ± 4.4	11.8 to 29.8	—	12
Rewarming	85.1 ± 6.2	35.2 ± 6.2	0.41	-122.7 ± 6.4	-7.7 to -9.6	-123 [8]	12
DP6							
Cooling	84.8 ± 17.4	44.4 ± 6.2	0.53	-125.0 ± 6.3	26.4 to 47.8	—	10
Rewarming	97.7 ± 15.9	39.7 ± 4.4	0.41	-120.8 ± 4.8	-7.81 to -10.3	-119 [12]	10
7.05 M DMSO							
Cooling	88.9 ± 15.9	58.7 ± 6.0	0.68	-128.7 ± 4.6	24.7 to 37.2	—	10
Rewarming	87.2 ± 13.7	52.2 ± 12.8	0.60	-126.0 ± 6.0	-8.7 to -11.5	-132 [10]	10

Asymptotic lines are best-fitted subject to a coefficient of determination (R^2) value of 0.995. β_{CG} and β_{GD} are the thermal expansion coefficients above and below the glass transition temperature, respectively. H is the cooling rate range in all experiments; and. $T_{G,DSC}$ is the glass transition temperature based on differential scanning calorimetry (DSC). The uncertainty range represents one standard deviation.

References

[1] G.M. Fahy, Biological effects of vitrification and devitrification, in: D.E. Pegg, A.M. Karow (Eds.), The Biophysics of Organ Preservation, Plenum Publishing Corp., New York, 1987, pp. 265–297.

[2] G.M. Fahy, D. Levy, S.E. Ali, Some emerging principles underlying the physical properties, biological actions, and utility of vitrification solutions, Cryobiology 24 (1987) 196–213.

[3] G.M. Fahy, J. Saur, R.J. Williams, Physical problems with the vitrification of large biological systems, Cryobiology 27 (1990) 492–510.

[4] J.L. Jimenez Rios, Y. Rabin, Thermal expansion of blood vessels in low cryogenic temperatures Part I: A new experimental device, Cryobiology (2005), in press, doi:10.1016/j.cryobiol.2005.12.005.

[5] C. Kroener, B.J. Luyet, Formation of cracks during the vitrification of glycerol solutions and disappearance of the cracks during rewarming, Biodynamica 10 (201) (1966) 47–52.

[6] B.J. Luyet, The vitrification of organic colloids and of protoplasm, Biodynamica 1 (29) (1937) 1–14.

[7] B.J. Luyet, G. Rapatz, An automatically regulated refrigeration system for small laboratory equipment and a microscope cooling stage, Biodynamica 7 (154) (1957) 337–345.

[8] P. Mehl, Nucleation and crystal growth in a vitrification solution tested for organ cryopreservation by vitrification, Cryobiology 30 (1993) 509–518.

[9] D.E. Pegg, M.C. Wusteman, S. Boylan, Fractures in cryopreserved elastic arteries, Cryobiology 34 (2) (1997) 183–192.

[10] J. Plitz, Y. Rabin, J.R. Walsh, The effect of thermal expansion of ingredients on the cocktails VS55 and DP6, Cell Preservation Technol. 2 (3) (2004) 215–226.

[11] Y. Rabin, J. Plitz, Thermal expansion of blood vessels and muscle specimens permeated with DMSO, DP6, and VS55 in cryogenic temperatures, Ann. Biomed. Eng. 33 (9) (2005) 1213–1228.

[12] Y. Rabin, M.J. Taylor, J.R. Walsh, S. Baicu, P.S. Steif, Cryomacroscopy of vitrification, Part I: a prototype and experimental observations on the cocktails VS55 and DP6, Cell Preservation Technol. 3 (3) (2005) 169–183.

[13] H. Scholtze, Glass, Springer-Verlag, New York, Berlin, Heidlberg, 1991.

[14] Y.C. Song, B.S. Khirabadi, F.G. Lightfoot, K.G.M. Brockbank, M.J. Taylor, Vitreous cryopreservation maintains the function of vascular grafts, Nat. Biotechnol. 18 (2000) 296–299.

[15] P.S. Steif, P.S.M. Palastro, C.R. Wen, S. Baicu, M.J. Taylor, Y. Rabin, Cryomacroscopy of vitrification, Part II: experimental observations and analysis of fracture formation in vitrified VS55 and DP6, Cell Preservation Technol. 3 (3) (2005) 184–200.

[16] M.J. Taylor, Sub-zero preservation and the prospect of long-term storage of multicellular tissues and organs, in: R.Y. Calne (Ed.), Transplantation Immunology: Clinical and Experimental, Oxford University Press, Oxford, New York, Tokyo, 1984, pp. 360–390.

[17] M.J. Taylor, Physico-chemical principles of low temperature biology, in: B.W.W. Grout, J.G. Morris (Eds.), The Effects of Low Temperatures on Biological System, Edward Arnold, London, 1987, pp. 3–71.